A comparison of different methods for predicting coal devolatilisation kinetics

A Arenillas, F. Rubiera, C. Pevida and J.J. Pis*

Instituto Nacional del Carbón, CSIC, Apartado 73, 33080 Oviedo, Spain

Abstract

Knowledge of the coal devolatilisation rate is of great importance because it exerts a marked effect on the overall combustion behaviour. Different approaches can be used to obtain the kinetics of the complex devolatilisation process. The simplest are empirical and employ global kinetics, where the Arrhenius expression is used to correlate rates of mass loss with temperature. In this study a high volatile bituminous coal was devolatilised at four different heating rates in a thermogravimetric analyser (TG) linked to a mass spectrometer (MS). As a first approach, the Arrhenius kinetic parameters (k and A) were calculated from the experimental results, assuming a single step process. Another approach is the distributed-activation energy model, which is more complex due to the assumption that devolatilisation occurs through several first-order reactions, which occur simultaneously. Recent advances in the understanding of coal structure have led to more fundamental approaches for modelling devolatilisation behaviour, such as network models. These are based on a physico-chemical description of coal structure. In the present study the FG-DVC (Functional Group-Depolymerisation, Vaporisation and Crosslinking) computer code was used as the network model and the FG-DVC predicted evolution of volatile compounds was compared with the experimental results. In addition, the predicted rate of mass loss from the FG-DVC model was used to obtain a third devolatilisation kinetic approach. The three methods were compared and discussed, with the experimental results as a reference.

Keywords: Coal pyrolysis; modelling; devolatilisation kinetics; TG-MS.

1. Introduction

The development of accurate predictive models for coal combustion or gasification, implies the knowledge of the rate and amount of volatiles released during the devolatilisation process. Volatiles can account for up to 70% of the coal mass loss during the overall combustion process. Pyrolysis conditions influence phenomena such as coal fluidity, coal softening and swelling, which affect the porosity and internal surface area of the resultant char. Thus, char reactivity depends on the thermal treatment undergone during coal devolatilisation. In addition, the pyrolysis variables control the product distribution of tar, char and gases, with ignition behaviour also being affected by the devolatilisation process. Likewise, carbon burnout depends on the amount of char remaining after devolatilisation, its intrinsic reactivity and particle morphology. It is clear then, that an accurate knowledge of the devolatilisation process is necessary to develop predictive models for coal combustion. However, pyrolysis is a very complex set of reactions, and accurate kinetics is not easy to obtain.

The chemistry of coal pyrolysis includes the decomposition of individual functional groups to produce light gas species, and the decomposition of the macromolecular network to produce smaller fragments, which can evolve as tar. Network decomposition is a complicated mixture of bridge breaking, crosslinking, hydrogen transfer, substitution reactions, concerted reactions, etc. The mass transport processes of the light species generated include: diffusion in the decomposing solid or liquid, vaporisation and gas phase diffusion, and pressure-driven convective transport. Transport can occur within the pores, by bubble movement or a combination of both [1].

As temperature is the most important parameter affecting pyrolysis, it might be useful to divide coal pyrolysis into three main temperature regions, [2]:

(i)   Temperature below 350-400ºC, where different processes take place prior to primary pyrolysis, i.e. disruption of hydrogen bonds, vaporisation and transport of the noncovalently bonded molecular phase.

(ii)   Between 400-700ºC, although this would depend on the nature of coal, the so-called primary pyrolysis takes place. This consists of a primary degradation, as a result of which the weakest bridges may break to produce molecular fragments. The fragments abstract hydrogen from the hydroaromatics or aliphatics, thus increasing the concentration of aromatic hydrogen [3]. These fragments will be released as tar if they are small enough to vaporise and be transported out of the char particle. Functional groups also decompose to release gases, mainly CO_2, light aliphatics, CH_4 and H_2O.

(iii)   At temperatures higher than 700ºC, the reactions that take place are mainly condensation of the carbon matrix, with the evolution of CO and H_2.

The aim of this work is to compile all of these reactions into a global kinetic model. Different approaches will be used: a global kinetic in a single reaction calculated from the experimental data, a distribution activation energy model, and the FG-DVC model which will be used to simulate the pyrolysis process and to generate data for a third devolatilisation kinetic approach. The results will be compared, with the experimental results as a reference.

2. Experimental

A high volatile bituminous coal, CA, from the north of Spain was used for this devolatilisation kinetics study. Ultimate analysis of this coal (wt%, dry and ash free basis) is as follows: 84.3 C, 5.6 H, 1.8 N, 1.6 S and 6.7 O. Proximate analysis (dry basis) yields 7.6 wt % ash and 37.7 wt % volatile matter.

Temperature-programmed pyrolysis experiments were performed in a thermobalance (TG), with a sample mass of about 10 mg, under an argon flow rate of 50 mL min^{-1}, at different heating rates (5, 15, 50 and 60ºC min^{-1}), from room temperature to 850ºC. The rate of mass loss was recorded as a function of temperature or time, and the different compounds evolved during pyrolysis were analysed by means of a mass spectrometer (MS), linked to the TG. The optimisation of this on-line equipment has been described elsewhere [4]. The results obtained at different heating rates were examined and different models were applied in order to obtain the kinetic constants for the 50ºC min^{-1} run.

There are a number of possible approaches for modelling the complex devolatilisation process. The simplest are empirical and employ global kinetics, where the Arrhenius expression is used to correlate rates of mass loss with temperature. These empirical methods can be divided into two groups: single or multiple step reactions.

The single step models [5-6] postulate that the devolatilisation process can be represented by the reaction:

$$coal \xrightarrow{\quad k_1 \quad} X\,(volatiles) + (1 - X)(char) \qquad (1)$$
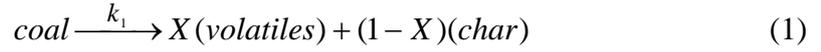
where X is the volatile fraction and the rate constant k_1 is given by the Arrhenius law:

$$k_1 = A_1 \times \exp\left[\frac{-E_1}{RT}\right] \qquad (2)$$

where A_1 is the frequency or pre-exponential factor in s^{-1}, E_1 is the activation energy in $J\ mol^{-1}$, R is the gas constant in $J\ K^{-1}\ mol$, and T is the absolute temperature in K.

In this work, as a first approach, a single-step kinetic model was used to determine the reaction constants from the measured reaction rates, dX/dt:

$$\frac{dX}{dt} = k_1 (X^* - X)^n \qquad (3)$$

where X^* represents the volatiles released at complete decomposition, and n is the reaction order. Different reaction orders were considered ($n = 0, 1, 2, 3$) for comparing the predicted values with the experimental ones.

Another approach is the distributed-activation energy model (DAEM), which is more complex due to the assumption that devolatilisation occurs through several first-order reactions, which occur simultaneously. When this model is applied to the change in total amount of volatiles, the following expression is obtained:

$$1 - \frac{X}{X^*} = \int_0^\infty \exp\left[-k_o \int_0^t e^{-E/RT}\,dt\right] f(E)\,dE \qquad (4)$$

where X represents the volatiles evolved at time t, X^* is the total volatile content of the coal, $f(E)$ is the distribution curve of the activation energy, and k_0 is the frequency factor. The distribution function $f(E)$ is defined to satisfy:

$$\int_0^\infty f(E)dE = 1 \qquad (5)$$

The focus of the analysis is the estimation of k_0 and $f(E)$. The distribution function $f(E)$ is generally assumed as a Gaussian distribution with a mean activation energy, E_0, and a standard deviation, σ. On the other hand, the frequency factor, k_0, is usually assumed to be a constant for all the reactions in order to simplify the analysis. However, the assignment of the Gaussian distribution to $f(E)$ does not always reflect the real situation. Furthermore, the assumption of a constant k_0 value may not be valid when $f(E)$ spreads over a wide range of E values. For this reason, an estimation of $f(E)$ and k_0 was achieved in this work from four sets of experiments, based on the method proposed by Miura [7-8], which does not assume any functional forms for $f(E)$ and k_0.

Recent advances in the understanding of coal structure have led to more fundamental approaches for modelling devolatilisation behaviour, such as network models, which are based on a physicochemical description of the coal structure. In the present study the FG-DVC (Functional Group – Depolymerisation, Vaporisation and Crosslinking) computer code was used as the network model. This model for coal thermal decomposition has six basic concepts [9]: functional groups, macromolecular network, network coordination number, bridge breaking, cross-linking and mass transport of tar. The first concept is based on the assumption that light gases are formed by the decomposition of certain functional groups in coal. The second concept is that coal consists of a macromolecular network, formed by fused aromatic clusters linked by

bridges, some of which are relatively weak. When heated, this network decomposes to produce smaller fragments. The lightest of the fragments evaporate to produce tar, while the heaviest ones form the metaplast. The third concept, the coordination number, describes the geometry of the network by specifying how many possible attachments exist per aromatic ring cluster. The coordination number controls the molecular weight distribution of the network fragments at a given extent of decomposition. Another important property of the network is the fraction of possible attachments that actually exist. During thermal decomposition, this fraction is determined by the rates of bridge breaking and cross-linking [10-12]. The factors which control how many of the bridges can break are the rate constant and the amount of hydrogen that can be donated to stabilise the free radicals that are formed when the bridges break. A competitive process with the bridge breaking is the retrogressive process of cross-linking. Cross-linking reactions appear to be related with the evolution of certain gases [13]. For low rank coals, cross-linking at low temperature (before bridge breaking) seems to be related with the evolution of carbon dioxide. A higher-temperature cross-linking event (following bridge breaking) seems to be related with the evolution of methane. At high temperatures, the evolution of hydrogen is also related with cross-linking in the form of aromatic ring condensation reactions. The final concept is that tar evolution is controlled by mass transport. The lightest fragments can leave the melting coal by evaporation into the light gas and tar species, while the heaviest fragments remain, forming the metaplast, which determines coal fluidity.

This network code takes into account many aspects related with the pyrolysis process and, therefore, gives a lot of information about the devolatilisation products. One of the

main advantages of the code is that it is applicable to any operating conditions (i.e. heating rate, residence time, and final temperature).

The predicted evolution of the volatile compounds obtained from the FG-DVC model was also compared with the experimental results. In addition, a set of devolatilisation kinetics assuming a single reaction of different orders (n = 0, 1, 2 and 3) was obtained from the predicted rate of mass loss obtained from the FG-DVC model.

3. Results and discussion

Figure 1 shows the mass loss curves obtained from the pyrolysis in the TG-MS system of the bituminous coal, CA, at different heating rates (5, 15, 50 and 60ºC min^{-1}). It can be observed that a difference of 10ºC min^{-1} in the heating rate does not affect the pyrolysis process very much. Thus, the curves obtained at 5 and 15ºC min^{-1} are very similar, and the same occurs with the curves at 50 and 60ºC min^{-1}. However, at higher heating rates (50-60ºC min^{-1}) the mass loss profiles shift to a higher temperature, and the final mass loss is lower than that at lower heating rates (5-15ºC min^{-1}). Table 1 shows some characteristic parameters of the devolatilisation process for the four heating rates. It can be seen that the temperature of the maximum rate of mass loss, Tmax, increases with the heating rate used during pyrolysis. On the other hand, the total volatile matter evolved, VM, and the temperature of volatile matter initiation, Ti, present a decreasing trend as the heating rate increases, as can be observed in Table 1. This could be due to the effect of heating rate on secondary reactions of the primary pyrolysis products (tar and high molecular weight compounds) as some authors have reported [14]. Thus, the char, tar and gas yields depend on the heating rate used during pyrolysis.

In general, kinetic studies are carried out under isothermal conditions. However, the use of non-isothermal conditions can be more useful if well-defined conditions are selected for investigating coal pyrolysis, in order to evaluate the kinetics during the initial and final phases of pyrolysis [15-16]. Such conditions can be obtained by heating the sample at a constant rate and using well-controlled operating conditions, i.e. a thermogravimetric analyser. In this work the experimental data obtained at 50ºC min^{-1} were chosen as the reference for all the kinetic calculations.

From the experimental evolution of mass loss with time, the reaction rate constant, k, can be calculated using Equation 3 for each selected reaction order. From a typical Arrhenius plot, $Ln\ k$ versus $1/T$, a linear relationship is obtained. From this plot, and according to Equation 2, the activation energy, Ea, and the pre-exponential factor, A, can be calculated. With these kinetic parameters (Ea and A), the reaction rate constant, k, can be recalculated using Equation 2, and hence the mass loss profile for each selected reaction order.

In this work, different reaction orders (n = 0, 1, 2 and 3) were considered and, in each case, the kinetic parameters (Ea and A) were calculated. The linear range in the Arrhenius plot changed slightly from one reaction order to another. Nevertheless, the main temperature range of volatile evolution (300-500ºC) was always taken into account in the calculations, and a regression factor, R^2, in the order of 0.98 was obtained in all cases. The results achieved from the experimental data are shown in Table 2. It can be observed that as the reaction order increases, the estimated Ea values also

increase and the *A* values decrease. In Figure 2 the experimental and calculated values of mass loss are compared.

It can be observed that the fit of predicted values for the different reaction orders in the main temperature range of volatile evolution (300-500ºC) is very good. The deviations are located at low temperatures (<300ºC) and mainly at high temperatures (>500ºC). A reaction order of n = 0, does not adequately represent the evolution of the mass loss at temperatures higher than 500ºC, as can be seen in Figure 2. This reaction order can therefore be rejected, which means that the volatile evolution is not constant with time. A reaction order of n = 3, gives a good representation of the last step in the pyrolysis process but it is worse in the main mass loss range, presenting a lower slope and thus indicating a slower process. This can be seen more clearly in Figure 3, where the rate of mass loss is presented versus temperature. It can be observed in this figure, that the temperature of the maximum rate of mass loss shifts to lower values as the reaction order increases. The peak, assuming a reaction order of n = 3, is wider and lower than that corresponding to the experimental data. The temperature of maximum mass loss of the experimental data lies between those obtained assuming n =2 and n = 3. This means that the pyrolysis process can be represented as a single reaction (Equation 1) but it is not an elementary reaction. Consequently, there is no correspondence between the stoichiometric and kinetic equations, and the reaction that can be observed, Equation 1, is the global effect of a sequence of elementary reactions.

Taking the above consideration into account, it is clear that the first approach for obtaining the kinetic parameters of pyrolysis as a single reaction presented some discrepancies with the experimental results. It also has the disadvantage that a new

calculation is needed for each run performed in the thermobalance, although with this method the calculations are simple and low time consuming. In addition, this approach could be useful when used as a first calculation step, and also for comparing the results of different samples or processes.

Figure 4 shows the typical Arrhenius plot obtained for the experimental data in this work, assuming a single third order reaction. The three main temperature ranges already mentioned, can be observed in this figure: T<400ºC where the main processes are disruption of hydrogen bonds, vaporisation and transport of the noncovalently bonded molecular phase; 400<T<700ºC where bridges-breaking takes place, and T>700ºC where the main reactions are condensation reactions. These temperature ranges are defined in Figure 4 as the three different slopes of the variation of *Ln k* with the reciprocal absolute temperature, *1/T*.

According to basic kinetics concepts, a variation of slope implies a variation of *Ea* with temperature and, thus, a variation in the mechanism that controls the reaction [17]. Usually, an increase in the slope in the Arrhenius plot (i.e. increase in the *Ea* value) implies that the controlling step changes from one mechanism to another. On the other hand, a decrease in the slope (i.e. decrease in the *Ea* value) means that the controlling step, in a series of reactions, changes from one reaction to another (Figure 5).

The distributed activation energy model, DAEM, includes several first-order reactions and might be a better approach for modelling the real process. In this work a DAEM was evaluated from the set of four experimental runs in the thermobalance, at different heating rates (5, 15, 50 and 60ºC min^{-1}). For each run, and assuming a first order

reaction, the nominal reaction rate constant k can be calculated at several identical volatile formation values but at different heating rates, and the Arrhenius plot can be considered [7]. In this case the activation energies were obtained from the Arrhenius plot at different levels of volatile formation. Thus, the same value of activation energy was obtained for the four heating rates, but its dependence on temperature varies with the operating conditions (i.e. heating rate). The distributed activation energy function, $f(E)$, is obtained by differentiating the volatile formation values from the activation energy values calculated. The frequency factor, k_0, is calculated using the following equation [8]:

$$k_0 = \frac{0.545 \; a \; E}{R \; T^2 e^{-E/RT}}$$

(6)

where a is the heating rate (K s^{-1}), T the temperature (K) and E the activation energy (J mol^{-1}).

The resultant function of activation energy is presented in Figure 6. It can be observed that $f(E)$ does not present the shape of a normal Gaussian distribution, the mean activation energy being 289.4 kJ mol^{-1}, which is the usual value for the devolatilisation of a bituminous coal, according to other authors [14, 18]. The k_0 obtained is a function of the activation energy, and presents nearly constant values with the heating rate, as can be seen in Figure 7. From these results and according to Equation 4, the volatile formation can be recalculated and compared with the experimental data. In this way, Figure 8 compares the mass loss profile of the experimental data and the estimation from the DAEM. It can be observed that the DAEM data reproduce the experiments in the TG very well.

The advantages of the DAEM is that it gives a good agreement with the real process and the $f(E)$ function, and it can be used for any heating rate used during pyrolysis in the same device. Furthermore, the frequency factor, k_0, is very similar for all the heating rates used in this work, so an average value can be used. Thus, only one set of calculations is needed and the mass loss profile can be predicted at any heating rate chosen. The main disadvantage is that the DAEM calculations are time-consuming.

The FG-DVC pyrolysis model is another useful tool for pyrolysis studies. It is very time-saving, it takes into account several reactions when modelling the pyrolysis process, and it does not need as many calculations as DAEM, because the program interpolates between a library of coals. The FG-DVC predictions are quite good, as can be seen in Figure 8 for the mass loss, and in Figure 3 for the rate of mass loss, although it presents a slight deviation at the beginning of the process. Figure 3 also shows that there is a very good correspondence between the temperature of maximum mass loss, in the FG-DVC profile, and the experimental one.

Another significant performance of the FG-DVC model is that it gives additional information such as the evolution of gaseous compounds or the composition of the pyrolysis products. As an example, the evolution of H_2 and CH_4 during the pyrolysis of coal CA at 50ºC min^{-1}, is presented in Figure 9 and compared with the profiles given by the FG-DVC code. Likewise, Figure 10 shows the elemental distribution (H, O, N and S) between the pyrolysis products, i.e. char, tar, paraphines + olephines, and gas, obtained from the FG-DVC model.

The FG-DVC code provides interesting information about the pyrolysis process and with reasonably accuracy. However, it does not give the kinetic parameters directly, although it provides the necessary data to calculate the kinetic parameters for individual gaseous compounds, tar formation or the total gaseous emissions, which can be interesting in particular cases [19]. Their calculation needs to be carried out from the mass loss curve predicted from FG-DVC, and assuming a single step reaction. In this work, a new set of calculations was performed, assuming single reactions of different orders (n = 0, 1, 2, and 3). The results obtained for *Ea* and *A* are shown in Table 3. The accuracy of the results was estimated to be as good as that presented in Figure 2 in the preliminary calculations.

Some mention should be made of the differences between the kinetics parameters calculated from the experimental data (Table 2) and the ones calculated from the predicted data of FG-DVC (Table 3). However, in this work, all of these calculated values should be considered only as fitting parameters, with no chemical significance.

4. Conclusions

From the results obtained in this work, it can be concluded that the approach of a single reaction, used in pyrolysis kinetic calculations, may be useful in the comparison of different samples or different pyrolysis processes. However, it does not fit the experimental results with great accuracy. The distribution of activated energy model was found to be the best option for representing the kinetic parameters and for reproducing mass loss with high accuracy. The use of FG-DVC presents additional benefits, as it is quick and easy to use, represents the real process in an acceptable way, and gives useful information about the pyrolysis process. Nevertheless, additional

calculations have to be performed to obtain kinetic parameters. Thus, a series of models are available for studying coal devolatilisation rates. The model finally chosen will depend on the particular needs of the study.

Acknowledgements

References

[1]   P.R. Solomon, M.A. Serio and E.M. Suuberg, Prog. Energy Combust. Sci., 18 (1992) 133.

[2]   W.R. Ladner, Fuel Processing Technology, 20 (1988) 207.

[3]   J.V. Ibarra and R. Moliner, J. Anal. Appl. Pyrolysis, 20 (1999) 171.

[4]   A. Arenillas, F. Rubiera and J.J. Pis, J. Anal. Appl. Pyrolysis, 50 (1999) 31.

[5]   S. Badzioch and P.G.W. Hawksley, Ind. Eng. Chem. Process Des. Dev., 9 (1970) 521.

[6]   P.R. Solomon, M.A. Serio, R.M. Carangelo and J.R. Markham, Fuel, 65 (1986) 182.

[7]   K. Miura, Energy & Fuels, 9 (1995) 302.

[8]   T. Maki, A. Takatsuno and K. Miura, Energy & Fuels, 11 (1997) 972.

[9]   P.R. Solomon, D.G. Hamblen, M.A. Serio, Z.Z. Yu and S. Charpenay, Fuel, 72 (1993) 469.

[10] E.M. Suuberg, P.E. Unger and J.W. Larsen, Energy & Fuels, 1 (1987) 305.

[11] B.C. Bockrath, E.G. Illig and W.D. Eassell-Bridger, Energy & Fuels, 1 (1987) 227.

[12] P.R. Solomon, M.A. Serio, G.V. Deshpande and E. Kroo, Energy & Fuels, 4 (1990) 42.

[13] E. M. Suuberg, D. Lee and J.W. Larsen, Fuel, 64 (1985) 1668.

[14] H. Jüntgen, Fuel, 63 (1984) 731.

[15] W. Wanzl, Fuel Processing Technology, 20 (1988) 317.

[16] M.J. Lazaro, R. Moliner and I. Suelves, J. Anal. Appl. Pyrolysis, 47 (1998) 111.

[17] O. Levenspiel, Chemical Reaction Engineering, John Wiley and Sons, Inc., New York, 1990, p. 35.

[18] K.H. van Heek, Ger. Chem. Eng., 7 (1984) 319.

[19] J.M. Jones, P.M. Patterson, M. Pourkashanian, A. Williams, A. Arenillas, F. Rubiera and J.J. Pis, Fuel, 78 (1999) 1171.

Table 1. Characteristic devolatilisation temperatures and volatile matter content for coal CA, obtained in the TG-MS at different heating rates.

Heating rate (°C min^{-1})	Tmax (°C)	Ti (°C)	VM (wt %, db)
5	449	335	39.7
15	455	337	41.9
50	484	273	37.6
60	486	272	36.3

Table 2. Kinetic parameters obtained by application of the model of single reaction to the mass loss experimental results.

Reaction order	Ea (kJ mol^{-1})	A (s^{-1})
0	57.2	208
1	74.4	114
2	94.1	95
3	94.1	4

Table 3. Kinetic parameters obtained by application of the model of single reaction to the mass loss predicted by the FG-DVC code.

Reaction order	Ea (kJ mol^{-1})	A (s^{-1})
0	108.4	637303
1	114.5	53637
2	126.1	11535
3	127.9	555
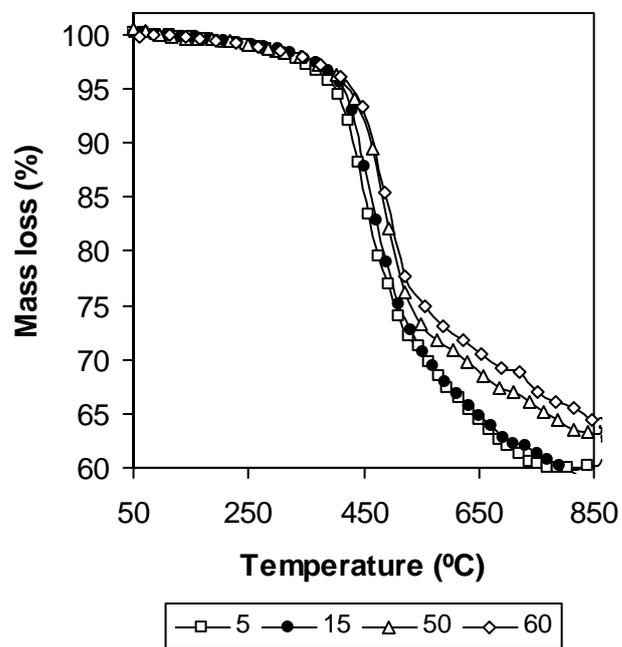
Figure 1. A. Arenillas et al. "A comparison of different methods.."
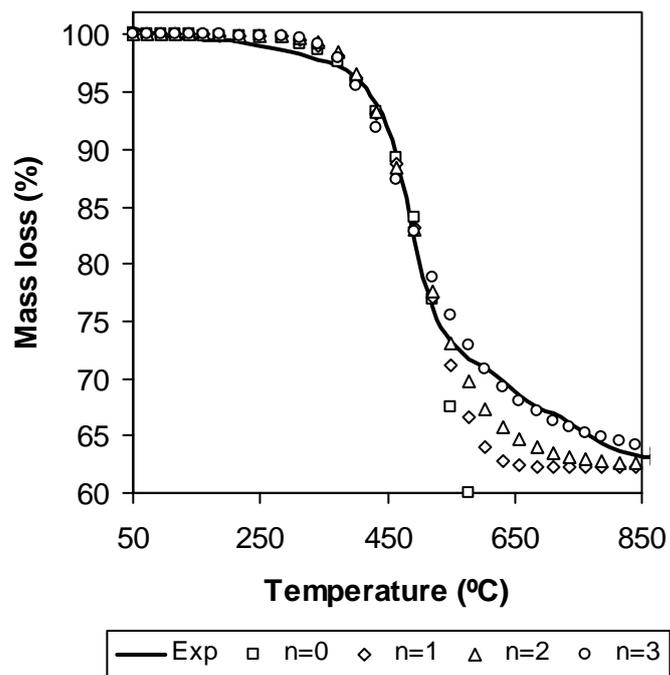
Figure 2. A. Arenillas et al. "A comparison of different methods.."
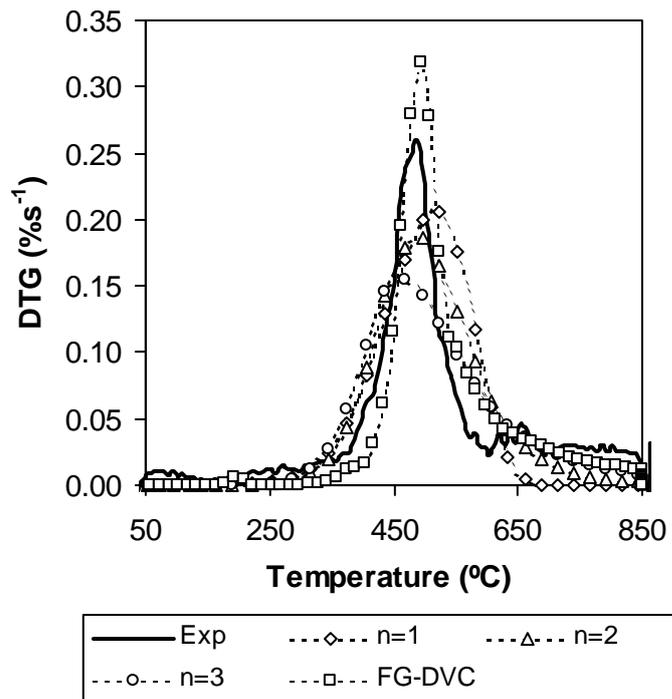
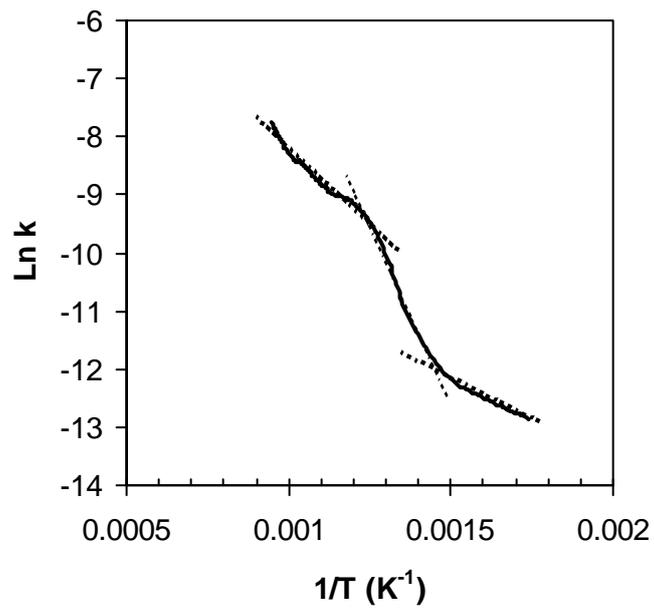Figure 3. A. Arenillas et al. "A comparison of different methods.."

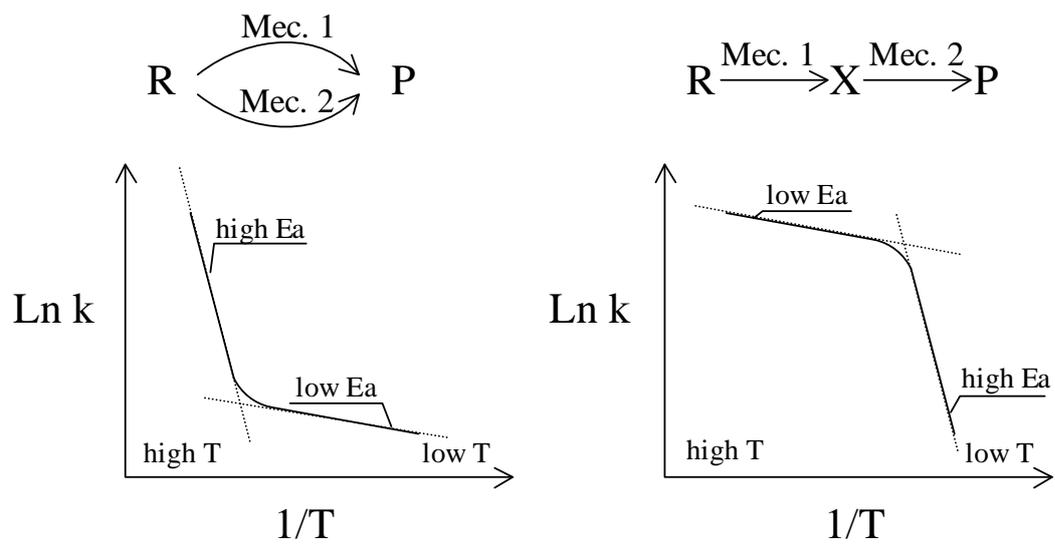Figure 4. A. Arenillas et al. "A comparison of different methods.."

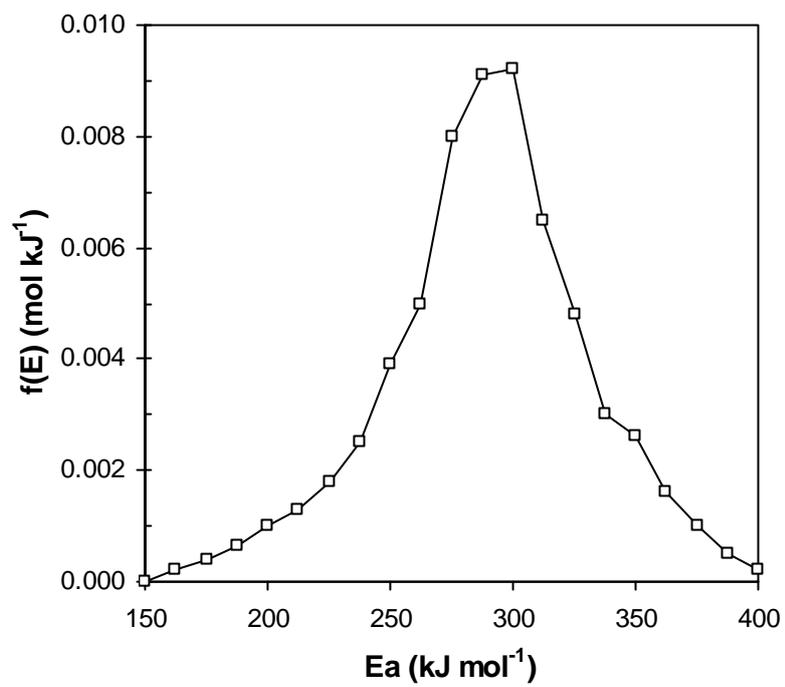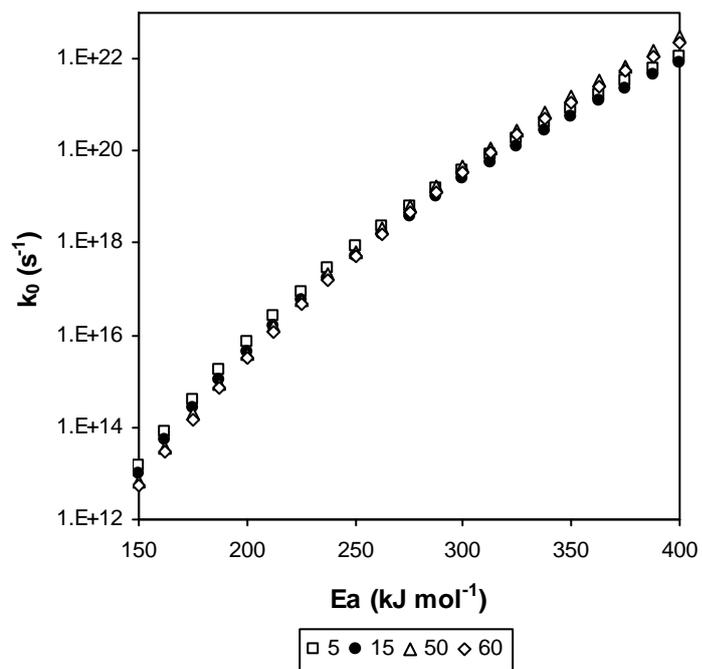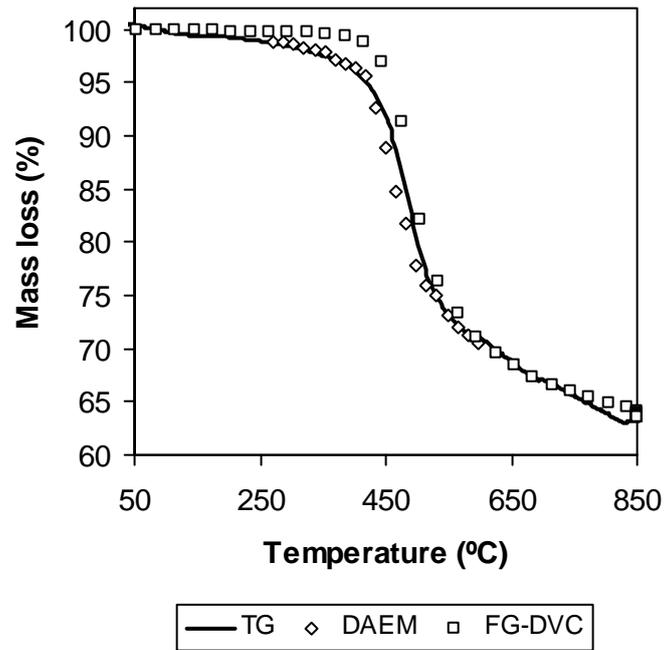Figure 5. A. Arenillas et al. "A comparison of different methods.."

Figure 6. A. Arenillas et al. "A comparison of different methods.."

Figure 7. A. Arenillas et al. "A comparison of different methods.."

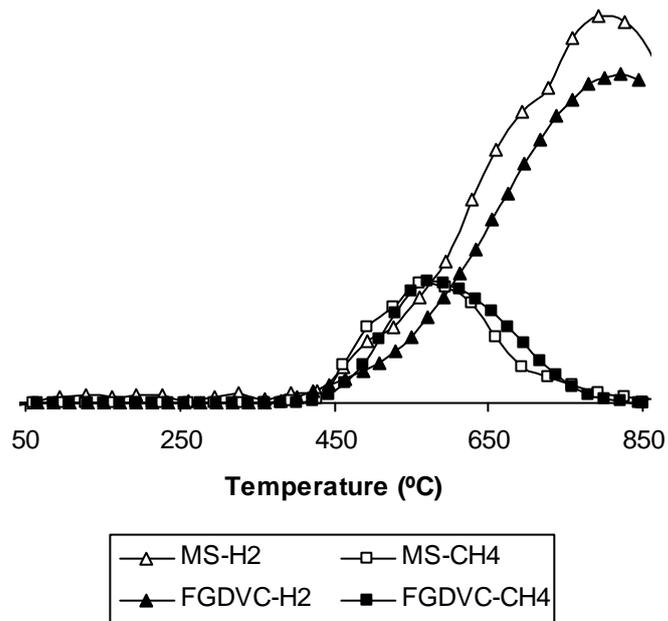Figure 8. A. Arenillas et al. "A comparison of different methods.."

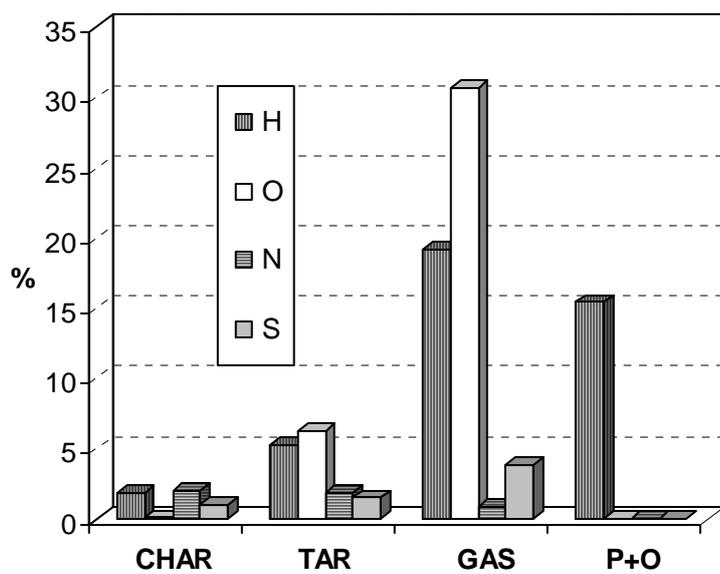Figure 9. A. Arenillas et al. "A comparison of different methods.."

Figure 10. A. Arenillas et al. "A comparison of different methods.."